Article

Discovery, Optimization, and Biological Evaluation of Sulfonamidoacetamides as an Inducer of Axon Regeneration

Jin-Mo Ku,[†] Kyuhee Park,[†] Jung Hun Lee,[†] Kyong Jin Cho,[‡] Yeon-Ju Nam,[†] Dae-Youn Jeong,[†] Yu-Han Kim,[§] SoonJung Kwon,[∥] Ju-Young Park,[∥] Jungeun Yang,[†] Tae-gyu Nam,[⊥] Sung-Hwa Yoon,[∥] Sangmee Ahn,*,[§] and Yongmun Choi*,[†]

[†]Bio-Center, Gyeonggi Institute of Science and Technology Promotion, 147 Gwanggyo-ro, Suwon, Korea 16229

[‡]Department of Ophthalmology, Medical College and [§]Department of Pharmacy, College of Pharmacy and Nanobiomedical Science, & BK21 PLUS NBM Global Research Center for Regenerative Medicine, Dankook University, 119 Dandae-ro, Cheonan, Korea 31116

[∥]Department of Applied Chemistry, Ajou University, 206 Worldcup-ro, Suwon, Korea 16499

[⊥]Department of Pharmacy, Hanyang University, 55 Hanyangdaehak-ro, Ansan, Korea 15588

S Supporting Information

ABSTRACT: Axon regeneration after injury in the central nervous system is hampered in part because if an age-dependent decline in the intrinsic axon growth potential, and one of the strategies to stimulate axon growth in injured neurons involves pharmacological manipulation of implicated signaling pathways. Here we report phenotypic cell-based screen of chemical libraries and structure−activity-guided optimization that resulted in the identification of compound **7p** which promotes neurite outgrowth of cultured primary neurons derived from the hippocampus, cerebral cortex, and retina. In an animal model of optic nerve injury, compound **7p** was shown to induce growth of GAP-43 positive axons, indicating that the in vitro neurite outgrowth activity of compound **7p** translates into stimulation of axon regeneration in vivo. Further optimization of compound **7p** and elucidation of the mechanisms by which it elicits axon regeneration in vivo will provide a rational basis for future efforts to enhance treatment strategies.

Compound **7p**
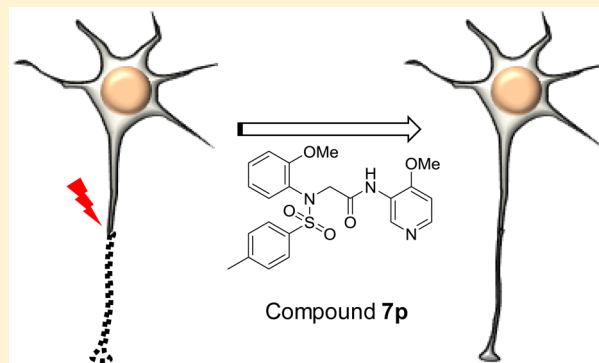
INTRODUCTION

The neurons in the adult central nervous system (CNS) fail to regenerate axons after injury, which accounts in part for the poor functional recovery in patients with traumatic and neurodegenerative diseases.[1] The failure of axon regeneration is attributable to a growth-inhibiting environment involving myelin-associated inhibitors (Nogo-A, myelin-associated glycoprotein, and oligodendrocyte/myelin glycoprotein) and glial scar at the injury site.[2] However, neutralizing and/or removing such inhibitory factors are insufficient to promote long-distance axon regeneration.[3] Adding to the complexity of inhibitory extrinsic factors is an age-dependent decline in the intrinsic axon growth potential: although the capacity of axon to elongate during development is robust, cell intrinsic mechanisms regulating axon growth are suppressed after the formation of functional synapses in the adult CNS and remain inactive even following traumatic injury.[4,5]

Recent years have seen some progress in understanding the mechanisms that lead to reactivation of cell intrinsic axon growth programs. The mechanisms involve an epigenetic regulation of gene transcription, development-dependent transcription factors, mTOR (mammalian target of rapamycin) and STAT3 (signal transducer and activator of transcription 3) signaling pathways, and manipulation of these cellular signaling pathways in conjunction with providing a permissive environment have been considered as therapeutic approaches to elicit axon growth in injured CNS neurons.[6−10]

Signaling pathways relevant to human diseases are likely to be amenable to small molecule intervention, and bioactive small molecules have proven to be valuable tools for exploring complex cellular processes.[11,12] Discovering such small molecules using unbiased screening approaches and identification of protein targets of the compounds should provide a rational basis for elucidating new drug targets and signaling pathways relevant to human diseases.[13,14] In this regard, phenotype-based small molecule screens involving axon elongation can provide an opportunity for pharmacological manipulation of previously unknown signaling factors that are implicated in cell intrinsic control of axon growth.[15] These

endeavors could bring forth novel therapeutic agents for the treatment of clinical conditions associated with a loss of axon.

In this study, in an effort to discover new pharmacological modalities to aid in axon regeneration, we employed phenotypic cell-based screens that allow visual assessment and quantitative measurement of neurite outgrowth in vitro. The phenotypic screening campaign and chemical modification efforts led to identification of compound **7p** that enhances neurite outgrowth in cultured primary neurons derived from the hippocampus, cerebral cortex, and retina and that induces optic nerve regeneration in an animal model of optic nerve injury. Although it needs to be determined how the compound stimulates axon growth in vivo, our results should provide further insight into the treatment strategies for clinical conditions associated with a loss of axon.

■ RESULTS AND DISCUSSION

Phenotypic Screens for Small Molecules That Stimulate Neurite Outgrowth. In an effort to discover synthetic small molecules that stimulate axon growth by targeting cell intrinsic mechanisms of axon elongation, we made use of neuronal differentiation of P19 embryonic carcinoma cells by neurogenic transcription factor NeuroD2 in the primary screen.[16,17] Upon expression of NeuroD2, P19 cells begin to sprout neurites that can be visually detected by indirect immunofluorescence with an antibody against neuron-specific class III β-tubulin.[18] We envisioned that the intrinsic mechanisms of axon growth in primary neurons can be recapitulated in the neurite outgrowth of P19-derived neuron-like cells.

We screened commercially available libraries of 170 000 synthetic small molecules from the DIVERSet libraries, kinase-directed libraries, PremiumSet library, and GPCR library (ChemBridge). The compounds were tested at a concentration of 10 μM in 384-well format for their ability to promote neurite outgrowth in P19 cells that were transiently transfected with a NeuroD2 cDNA construct. The compounds that enhance neurite outgrowth greater than twofold as compared with neurite outgrowth in DMSO-treated cells were selected, and we were able to confirm the activity of 185 compounds (0.11% hit rate). Then, the hit compounds were subject to a secondary screen that involves axon elongation in rat primary hippocampal neurons. The primary hippocampal neurons have been extensively used as a cellular system to study neuritogenesis,[19,20] and we tested the hit compounds that enhance neurite outgrowth in P19 cells to see whether they can stimulate neurite elongation in the neuronal context. Interestingly, the secondary screen yielded a set of compounds that share a common chemical scaffold containing a core substructure of sulfonamido acetamide, and compound **1** was most potent among the analogs (Figure 1). The neurite elongation activity of compound **1** reached a plateau at concentrations between 10 and 20 μM (~3 fold higher than control), and it lost neurite elongation activity below 1 μM. Similarly, compound **1** was able to enhance neurite elongation in assay with primary cortical neurons with a similar potency as shown in primary hippocampus neurons (data not shown).

Chemistry. Compound **1** exhibited in vitro limited water solubility and poor metabolic stability (half-life in liver S9 fraction), indicating that compound **1** is not an appropriate candidate for evaluation in vivo. To address these deficiencies, we initiated structure−activity-guided optimization using the neurite elongation of primary cortical neurons.
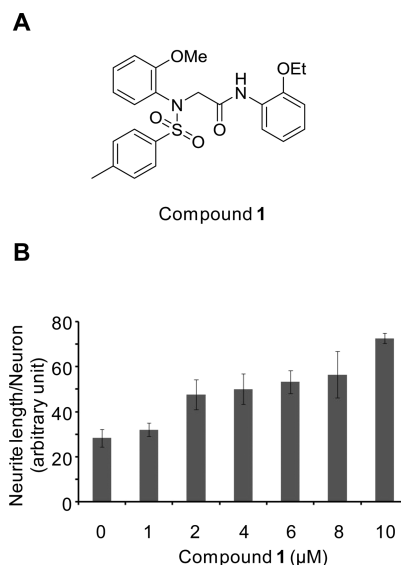
A

Compound **1**

B

Figure 1. (A) Chemical structure of compound **1**. (B) Neurite outgrowth activity of compound **1**. The primary neurons were stained with an anti-β-III tubulin antibody, and wide-field fluorescence images from four fields in each well of 384-well plate were acquired. The neurite total length divided by the number of neuron is shown. Each column represents the mean ± SD, $n = 3$.

We sectioned the chemical structure of the compound for chemical modification as shown in Figure 2 and planned three
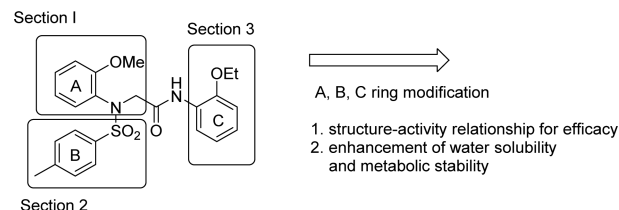

Figure 2. Strategy of structural modification of compound **1**.

synthesis routes in order to synthesize the derivatives of compound **1** as shown in Figure 3. In route A, compound **A** bearing R_1 and R_2 was used to introduce an aromatic ring or a heteroaromatic ring that include various substituents in section 3 of compound **1**. Compound **B** was obtained through hydrolysis of compound **A** and compound **B** reacted with diverse amine (**C**) to synthesize compound **D**. Synthesis route B was advantageous for fixing R_1 and R_3 and changing the structure of R_2. Compound **E** was synthesized by substitution reaction, and then reacted with various sulfonyl chloride compounds (**F**) along with the diversity of R_2. There is a limitation that secondary amine (−NH−) and nitrogen (−NHCO−) of amide in compound **E** competitively reacted with alkyl halide or acyl halide to produce mixtures. Alternatively, we chose route C to minimize production of the mixtures (tertiary amine and secondary amide) as mentioned above. Amine compounds bearing various substituents (R_1) reacted with arylsulfonyl chloride, acyl chloride, and alkyl chloride for compound **G**, which was substituted with compound **H** to afford the compound **D**. As mentioned above, we could avoid competitive reactions of secondary amine (−NH−) and amide (−NHCO−) of compound **E** because R_2 was introduced in advance.
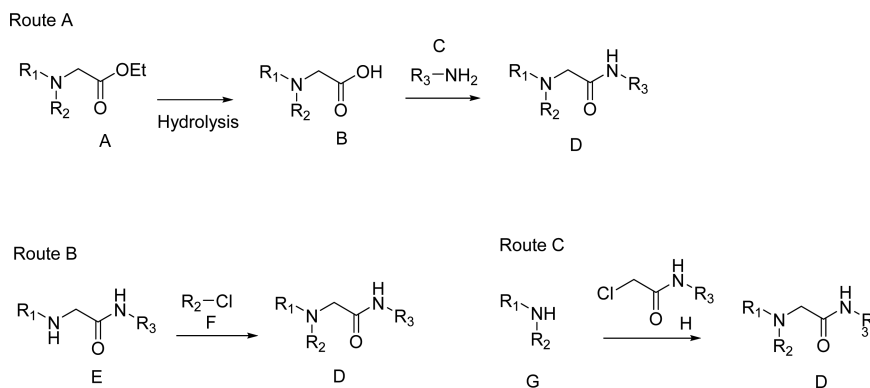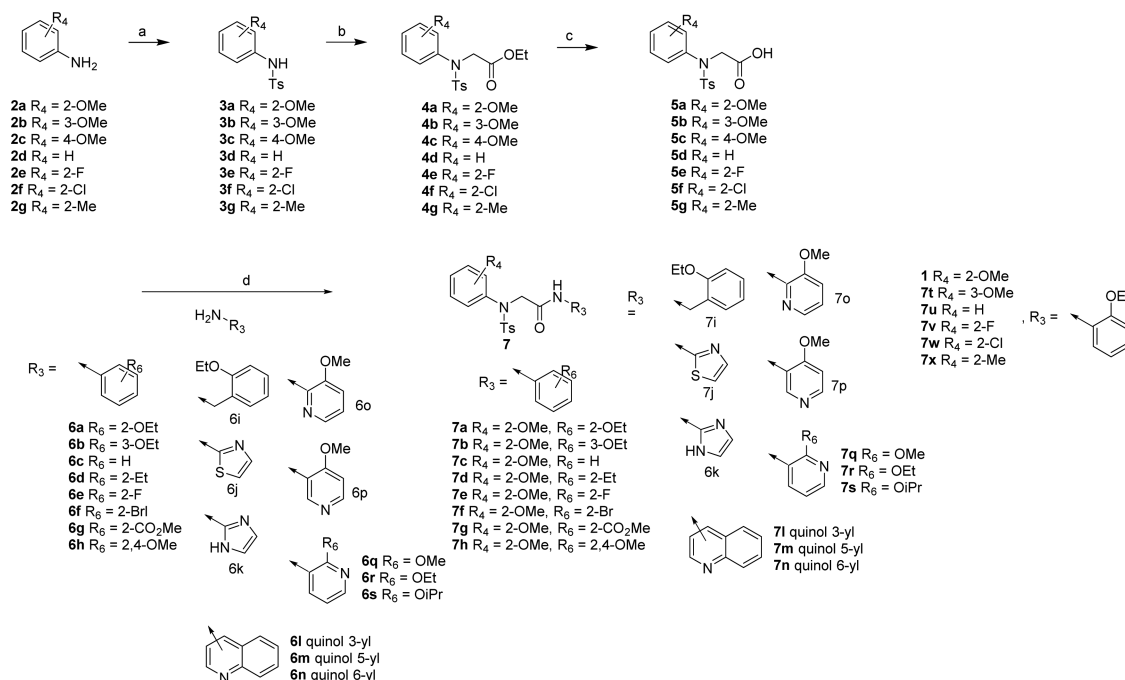
Figure 3. Synthesis routes for structural modifications of compound **1** and its derivatives.

Scheme 1. Synthesis of Compounds 7a–x through Synthesis Route A[a]

[a](a) Tosyl chloride, K₂CO₃, DMF, rt, 2 h; (b) ethyl bromoacetate, K₂CO₃, DMF, rt, 12 h ; (c) 2.5 M NaOH solution, THF, reflux, 6 h; and (d) HATU, triethylamine, DMF, rt, 2 h.
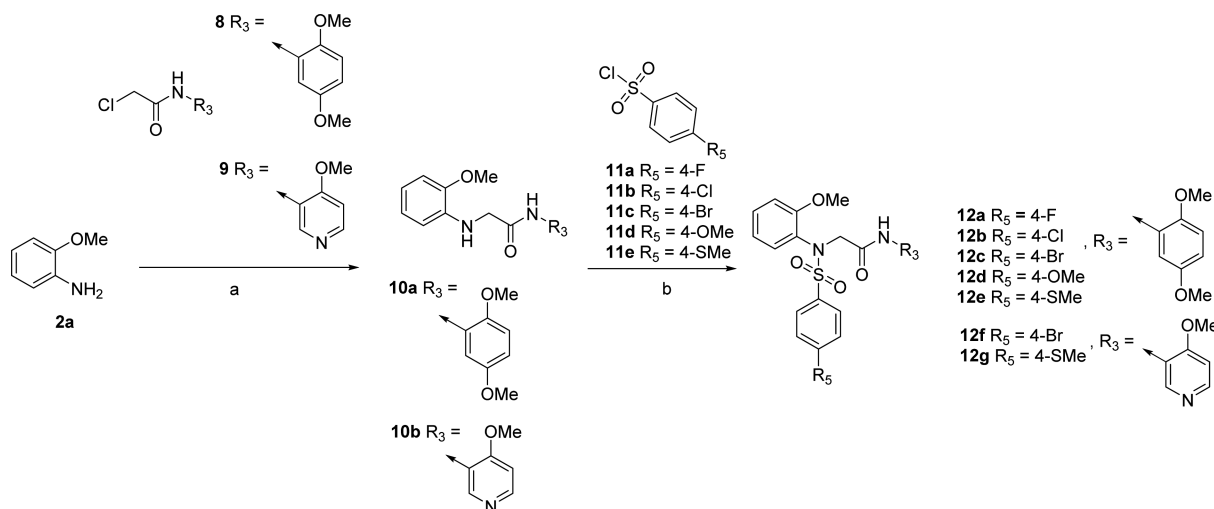
The synthesis of compounds **7a–x** through synthesis route A is described in Scheme 1. Compounds **2a–g** were selected as starting materials and reacted with toluenesufonyl chloride to synthesize *N*-toluenesulfonamides (compounds **3a–g**). Substitutions of compounds **3a–g** with ethyl bromoacetate afforded compounds **4a–g**, which was followed by base-catalyzed hydrolysis to obtain compounds **5a–g**. HATU (1-[bis(dimethylamino)methylene]-1*H*-1,2,3-triazolo[4,5-*b*]-pyridinium 3-oxid hexafluorophosphate) was chosen to produce an active ester to conduct amide coupling of various amines (compounds **6a–t**) and carboxylic acid (compound **5a–g**) for compounds **7a–x**.

Compounds **12a–g** bearing 2-methoxy in R₃ and 2,4-dimethoxyphenyl or 4-methoxy-pyridin-3-yl in R₆ were synthesized by reaction of compounds **10a** and **10b** with various benzenesulfonyl chloride through synthesis route B. Substitution reactions of compound **2a** with compounds **8** and **9** were carried out for compounds **10a** and **10b**, which was followed by reaction with arylsufonyl chlorides (**11a–e**) to

synthesize compounds **12a–g** having diverse substituents in the C ring (Scheme 2).

Compounds **17** and **18** were synthesized for substitution of sulfonamide into amide (−CONH−) or alkyl (−CH₂−) as linkers in section 2 via synthesis route C. Compound **2a** was reacted with chlorobenzoyl chloride (**13**) and 4-methylbenzyl chloride (**14**), respectively, afforded N-acylated compound **15** and N-alkylated compound **16**, which were reacted with compound **8** to synthesize compounds **17** and **18**. At the beginning, we tried to synthesize compounds **17** and **18** through synthesis route B; however, the chemical yields were low because of a competitive reaction of two nucleophilic nitrogens of secondary amine and amide in compound **E**. Alternatively, synthesis route C was required and showed no undesired products (Scheme 3).

The neurite outgrowth activities of the compounds bearing the various substituents of ring C and heteroaromatic system in section 3 were summarized in Table 1. First, we modified section 3 to find the effective functional group on ring C. The

Scheme 2. Synthesis of Compounds 12a−g via Synthesis Route B[a]

[a](a) **8** or **9**, K$_2$CO$_3$, DMF, 80 °C, 2 h; (b) pyridine, DCM, rt, 3 h.

Scheme 3. Synthesis of Compounds 17 and 18 Synthesis Route C[a]
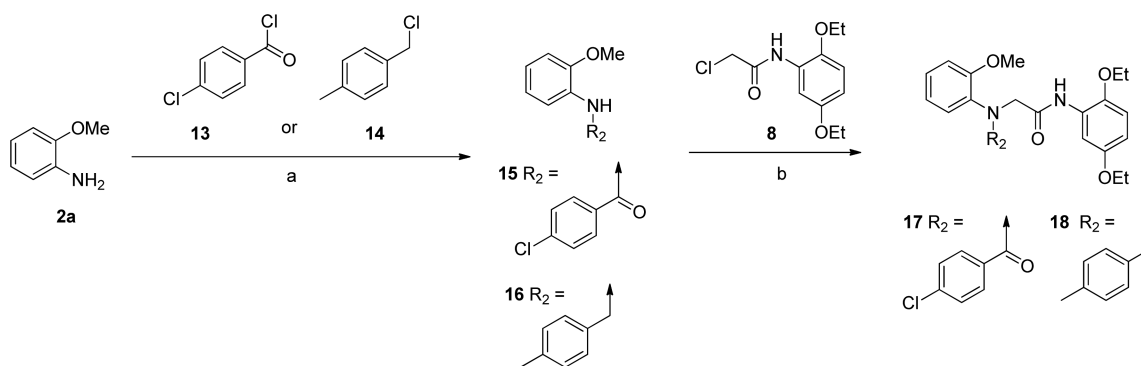
[a](a) **13** or **14**, K$_2$CO$_3$, DMF, rt, 2 h; (b) **8**, K$_2$CO$_3$, DMF, 80 °C, 2 h.

Table 1. Neurite Outgrowth Activity of R$_3$- and R$_6$-Modified Compounds
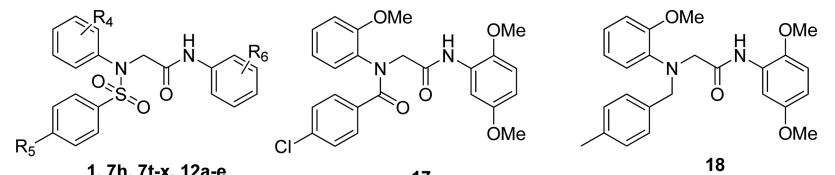
entry	compound	R$_6$	fold increase at 10 μM, compared to DMSO	synthesis route
1	**1**	2-ethoxy	3.2 ± 0.4[a]	B
2	**7b**	3-ethoxy	1.8 ± 0.3	[b]
3	**7c**	H	2.0 ± 0.1	B
4	**7d**	2-ethyl	0.8 ± 0.1	B
5	**7e**	2-fluoro	2.1 ± 0.2	B
6	**7f**	2-bromo	2.1 ± 0.2	B
7	**7g**	2-methoxycarbonyl	3.0 ± 0.4	[b]
8	**7h**	2,4-dimethoxy	2.7 ± 0.3	[b]
9	**7i**	depicted above	cytotoxic	A
10	**7j**	depicted above	cytotoxic	A
11	**7k**	depicted above	cytotoxic	A

[a]The data are shown as mean ± standard deviation, n = 3.
[b]Commercially available compound was used.

directing effect of the substituents on ring C was mostly shown in the ortho position (Table 1, entries 1 and 2) and the ethoxy group, an electron-donating group, confer better outgrowth activity, compared to an electron-withdrawing group, such as halogen and methoxycarbonyl (Table 1, entries 1−8). Replacement of the 2-ethoxyphenyl on ring C of compound **1** with 2-ethoxybenzyl yielded compound **7i** where ring C was placed far away from the basic frame because of the insertion of methylene. However, replacement of 2-ethoxyphenyl with imidazole or thiazole yielded compounds that exhibited cytotoxicity in neurite outgrowth assay with primary cortical neurons (Table 1, entries 9−11).

We next investigated the structure−activity relationship between substituents in R$_4$ of ring A and R$_5$ of ring B along with 2-ethoxy or 2,4-dimethoxy in R$_6$ of ring C (Table 2). First, the activity of the compounds that adopted a methoxy group in ortho or meta position in R$_4$ was compared, and it was revealed that the meta-substituted compounds exhibited less activity as compared to compound **1** (Table 2, entries 1 and 2). There was no significant difference in neurite outgrowth activity depending on electron-donating/-withdrawing groups on ring A (Table 2, entries 1 and 3−6). Because 2,4-dimthoxy group in R$_6$ presented activity similar to that of compound **1**, chemical modification was shifted to R$_5$ in ring B. The activities of halogen-substituted compounds were higher than that of

Table 2. Neurite Outgrowth Activities of R_4- and R_5-Modified Compounds

entry	compound	R_4	R_5	R_6	fold increase at 10 μM, compared to DMSO	synthesis route
1	**1**	2-methoxy	CH_3	2-ethoxy	3.2 ± 0.4^a	B
2	**7t**	3-methoxy	CH_3	2-ethoxy	3.1 ± 0.3	B
3	**7u**	H	CH_3	2-ethoxy	2.5 ± 0.3	B
4	**7v**	2-fluoro	CH_3	2-ethoxy	2.9 ± 0.3	B
5	**7w**	2-chloro	CH_3	2-ethoxy	2.6 ± 0.2	B
6	**7x**	2-methyl	CH_3	2-ethoxy	2.6 ± 0.3	B
7	**7h**	2-methoxy	CH_3	2,4-dimethoxy	2.7 ± 0.4	C
8	**12a**	2-methoxy	F	2,4-dimethoxy	2.5 ± 0.2	C
9	**12b**	2-methoxy	Cl	2,4-dimethoxy	4.2 ± 0.5	C
10	**12c**	2-methoxy	Br	2,4-dimethoxy	5.0 ± 0.4	C
11	**12d**	2-methoxy	MeO	2,4-dimethoxy	2.3 ± 0.2	C
12	**12e**	2-methoxy	MeS	2,4-dimethoxy	3.2 ± 0.4	B
13	**17**	depicted above			1.0 ± 0.1	B
14	**18**	depicted above			cytotoxic	B

^{a}The data are shown as mean $\pm$ standard deviation, $n = 3$.

compound **12d** in that 4-methoxy was substituted for methyl of R_5 (Table 2, entries 8−11). Among them, the neurite outgrowth activity of 4-bromo-substituted compound **12c** was fivefold higher than that of DMSO (Table 2, entry 10). We synthesized compounds **17** and **18** bearing 4-chlorobenzoyl and methylbenzyl in order to test whether the sulfonamide in section 2 is a structural feature necessary to impart activity; however, the results showed that replacements of the sulfonamide residue led to a complete loss of neurite outgrowth activity or yielded compounds that exhibits cytotoxicity (Table 2, entries 14 and 15).

We measured the metabolic stability in mouse liver S9 fraction of compounds **1**, **7g**, **12b**, and **12d** whose neurite outgrowth activity was higher than that of DMSO. Unfortunately, when the selected compounds were incubated in the presence of isolated mouse liver S9 fraction for 30 min, the residual rates were 0.3−0.7%, suggesting very low metabolic stability. One of the strategies for improving the metabolic stability of the compound is to reduce the overall lipophilicity (e.g., log P and log D). Because the binding site of metabolizing enzyme is lipophilic, lipophilic molecules could be accepted more readily to the binding site of enzymes.[21] Thus, we designed compounds with higher metabolic stability and synthesized compounds introducing pyridine or quinoline, as shown in Table 3. The neurite outgrowth activities were different depending on the substituted positions of quinoline; in particular, compound **7l** showed the highest activity (Table 3, entries 1−3). Replacement of R_3 with pyridine derivatives resulted in compounds with varied potency depending on the position of nitrogen; the most potent one was compound **7p** (Table 3, entries 4−6). As expected, the lipophilicity of compound **7p** (log P = 2.43) bearing the pyridyl amide was reduced when compared to that of compound **1** (log P = 3.76); hence, the metabolic stability of compound **7p** (remaining compound, 61.2%) was remarkably enhanced relative to compound **1** (remaining compound, 0.7%) (Table 4). In addition, it was assumed that the small alkoxy group on

pyridine was more adequate with regards to the neurite outgrowth activity (Table 3, entries 6−8). Further modification of compound **7p** by introducing 4-methylthio or 4-bromo substituent in section 2 did not adversely affect its ability to enhance neurite outgrowth of primary cortical neurons (Table 3, entries 9−10).

Taken together, the structure−activity-guided optimization efforts led to identification of a subset of compounds that exhibit improved neurite outgrowth activity and water solubility as compared to those of compound **1**; compound **7p** was best among the derivatives because it also exhibited improved metabolic stability relative to compound **1**.

Effect of Compound 7p on Optic Nerve Regeneration. We discovered that compound **1** and its derivatives demonstrated the ability to stimulate neurite outgrowth of cultured primary neurons derived from hippocampus and cerebral cortex in the brain of rat E18. The in vitro results raised the question of whether such compounds can stimulate axon outgrowth and produce desired biological outcome such as axon regeneration in CNS injury site. To address the question, we first tested compound **7p** for its ability to stimulate axon growth of retina neuronal cells in vitro and then employed an animal model of optic nerve injury to test compound **7p** in vivo.

The retina neuronal cells prepared as described in the Experimental Section were treated with compound **7p** at concentrations between 2 and 20 μM. After a 72 h incubation, the cells were fixed with paraformaldehyde and stained with an anti-neurofilament antibody (SMI-312) to detect axons (Figure 4A,B). Axonal outgrowth was quantified by counting the number of neuronal cells with axon length <50 μm, axon length of 50−100 μm, axon length of 100−200 μm, or axon length longer than 200 μm. Although the cultures were purified partially, we were able to select retinal ganglion cells (RGCs) by cell size and morphology, and the cells bigger than 10 μm in cell body diameter were counted. As shown in Figure 4C, the

Table 3. Structural Modification of Compounds 1 and 12c for Improving Metabolic Stability

(General structure: 2-OMe phenyl attached to N; N bears a sulfonyl group with a 4-R_5-phenyl; N also bears CH$_2$C(=O)NH–R_3)

7l-s, 12f-g

Entry	Compound	R_3	R_5	Fold increase at 10 μM, compared to DMSO	Synthetic route
1	**7l**	quinolin-3-ylmethyl	CH_3	3.6 ± 0.3^{a}	A
2	**7m**	isoquinolin-5-ylmethyl	CH_3	1.3 ± 0.1	A
3	**7n**	quinolin-6-ylmethyl	CH_3	1.0 ± 0.1	A
4	**7o**	(2-OMe-pyridin-3-yl)methyl	CH_3	1.6 ± 0.1	A
5	**7p**	(4-OMe-pyridin-3-yl)methyl	CH_3	4.2 ± 0.5	A
6	**7q**	(2-OMe-pyridin-3-yl)methyl	CH_3	2.8 ± 0.3	B
7	**7r**	(2-OEt-pyridin-3-yl)methyl	CH_3	2.1 ± 0.1	A
8	**7s**	(2-OiPr-pyridin-3-yl)methyl	CH_3	2.3 ± 0.2	A
9	**12f**	(4-OMe-pyridin-3-yl)methyl	CH_3S	3.9 ± 0.3	A
10	**12g**	(4-OMe-pyridin-3-yl)methyl	Br	3.7 ± 0.4	A

^{a}The data are shown as mean $\pm$ standard deviation, $n = 3$.

Table 4. Metabolic Stability in Mouse Liver S9 Fraction

entry	compound	compound remaining (%)	log P^{c}
1	**1**	0.7	3.76
2	**7g**	0.3	3.37
3	**12b**	0.4	3.37
4	**12d**	0.4	2.69
5	**7p**	61.2	2.43
6	acetaminophen^{a}	97.7	
7	verapamil^{b}	23.1	

^{a}Acetaminophen, positive control, was not metabolized in Phase I. ^{b}Verapamil, negative control, was metabolized in Phase I. ^{c}log P was calculated by Chemdraw, ver. 12.

axonal growth stimulatory effect of compound **7p** was evident in all range of length and was most prominent at 10 μM.

To examine whether compound **7p** was able to stimulate axonal outgrowth of RGCs in an animal model of optic nerve injury, the crushed optic nerves in the injury model were treated with either PBS or compound **7p** (0.22 μg per eye) for 3 weeks. Then, the animals were sacrificed, and optic nerve sections were stained with an anti-GAP43 antibody to visualize growing axons. As shown in Figure 5A, the axons of optic nerves from animals treated with compound **7p** were significantly extended beyond the lesion epicenter as compared to those from the sham-control animals treated with PBS. The differences in the number of GAP-43 positive axons were evident in all cases of measurements at 500, 1000, and 1500 μm distal to the crush center (Figure 5B) but were statistically significant beyond 1500 μm (injured, 0.22 ± 0.081; injured + **7p**, 0.70 ± 0.20) as determined by quantification of GAP-43 positive axons.

■ **CONCLUSIONS**

An approach to activate cell-intrinsic mechanisms regulating axon growth in the adult CNS is likely to contribute to functional recovery following traumatic injury. Upon screening chemical libraries of 170 000 synthetic small molecules for those that stimulate neurite outgrowth of P19-derived neuron-like cells, we discovered a promising hit (compound **1**) that is also capable of stimulating neurite outgrowth of cultured primary neurons. The structure–activity-guided optimization and the efforts to improve metabolic stability of compound **1** resulted in the identification of compound **7p** with properties more suitable for in vivo studies. It is of note that the in vitro neurite outgrowth activity of compound **7p** translates into stimulation of axon regeneration in an animal model of optic nerve injury. Further optimization of compound **7p** and elucidating the mechanisms by which compound **7p** elicits
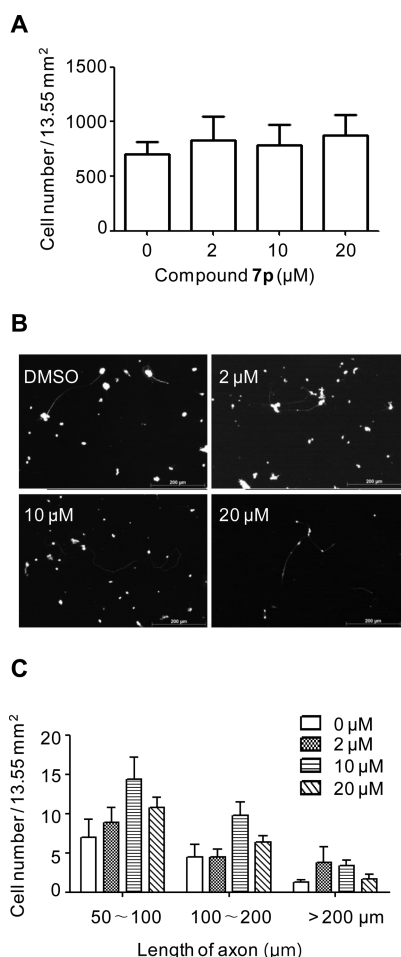
Figure 4. Effect of compound **7p** on the viability and axonal growth of cultured retina neuronal cells. The cells were treated with compound **7p** (2–20 μM) for 72 h, and then the viability and axonal growth were evaluated. (A) Total numbers of live cells in nine consecutive nonoverlapping microscopic fields were counted. No significant difference was found ($n = 3$). (B) The cells were immunostained with an antineurofilament antibody to detect axons, and representative images are shown. (C) Axonal growth was measured as described in the Experimental Section after staining the culture with an antineurofilament antibody. Each column represents the mean $\pm$ SEM, $n = 9$ (3 independent experiments).

axon regeneration in vivo will provide a rational basis for future efforts to enhance treatment strategies.

■ EXPERIMENTAL SECTION

P19 Cell Culture and Chemical Treatment. P19 embryonic carcinoma cells (6×10^6/10 cm dish) were transfected with 10 μg of DNA construct encoding NeuroD2 by using FuGENE HD. At 12 hr after transfection, the cells were trypsinized and replated at a density of 8000 cells/well to a 384-well plate in MEM (minimum essential medium) containing 5% FBS, 1 mM sodium pyruvate, and 2 mM glutamate. After a 24 h incubation, the cells were treated with compounds for 48 h, and then beta III tubulin was visualized by indirect immunofluorescence. The chemical libraries used in this work were purchased from ChemBridge Corporation (San Diego, CA, USA).

Animal Housing and Ethics. The animal study was approved by the Animal Ethical Committee of Gyeonggi Institute of Science & Technology Promotion and Dankook University, and carried out in accordance with guidelines from KFDA (Korea Food and Drug Administration) and Animal and Plant Quarantine Agency in Korea.
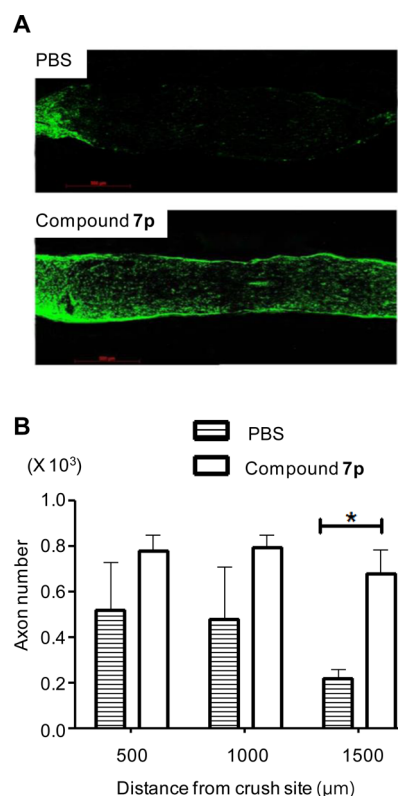

Figure 5. Compound **7p** promoted regeneration of the crushed optic nerves. (A) The rat optic nerves were crushed and treated with either PBS or compound **7p**, and then longitudinal sections of rat optic nerves were immunostained with an anti-GAP43 antibody. Fluorescence images show nerve fiber identified by GAP-43 immunoreactivity. (B) The numbers of axons at indicated sites were counted, and all values are shown as mean $\pm$ standard error of the mean, $n = 4$ (11–15 sections from 4 rats, each), *, $p < 0.05$.

Cell Culture of Primary Neurons. Entire forebrains were dissected from embryonic day 18 (E18) embryos of Sprague–Dawley (SD) rats as described with minor modification.[22] In brief, the skull covering the brain was cut and opened with microscissors, and the brain was transferred to a clean dish with ice-cold Hank's buffered salt solution (HBSS). The meninges were teased off with microforceps, and hippocampus and cerebral cortex were collected separately in HBSS. After being centrifuged at $100g$ for 1 min, they were resuspended in Neurobasal medium containing serum-free supplement (B27) and 2 mM glutamate and then were triturated approximately 30 times with a 1 mL micropipette tip to achieve a single-cell suspension. The cells were washed twice with Neurobasal medium containing B27 and 2 mM glutamate, passed through a 40 μm cell strainer, and then seeded onto 384-well plates at a density of 2000 cells/well. After a 24 h incubation, the cells were treated with compounds for 48 h, and then beta III tubulin was visualized by indirect immunofluorescence.

RGCs were obtained from the postnatal day 7 (P7) SD rats and maintained in Dulbecco's phosphate-buffered saline (DPBS) with 0.5% bovine serum albumin (BSA, MP, Cellect BSA). RGCs separation was done by using a RGC isolation kit (Miltenyi Biotec; Auburn, CA). The RGCs were seeded on 18 mm cover glass (Deckglaser) in 12-well plates (Costar, Corning, NY), which had been precoated with poly-D-lysine (20 μg/mL) followed by laminin (10 μg/mL) in Dulbecco's modified Eagle's medium (DMEM) at a density of 200 000 cells/well. At 2 h after plating, RGCs were treated with various doses (0, 2, 10, and 20 μM) of compound **7p** and maintained for 3 days.

Indirect Immunofluorescence. Fixed cells were washed with PBS and permeabilized with 0.25% Triton X-100 in PBS for 8 min. Primary and secondary antibodies were diluted in PBS containing 5%

BSA and used for staining. The antibodies are as follows: 0.5 μg/mL of mouse anti-β III tubulin (Covance) and 2 μg/mL Alexa Fluor 488 goat anti-mouse IgG (Invitrogen). 4′,6-Diamidino-2-phenylindole (DAPI) was used to stain the nucleus. Confocal fluorescence images were acquired using a LSM700 with Zen software (Carl Zeiss).

The cultured retina neuronal cells were washed with 0.1 M PBS, fixed with 4% paraformaldehyde (PFA) prepared in 0.1 M PBS for 15 min at room temperature, and washed again with 0.1 M PBS twice for 5 min. Nonspecific protein binding was blocked by incubation with 1% BSA and 3% goat serum (Vector Laboratories, Burlingame, CA) prepared in 0.1 M PBS containing 0.1% Triton X-100 (Sigma) for 60 min. First, cells were incubated with primary antineurofilament antibody (SMI312 Monoclonal, 1:400, Covance) antibody for overnight at 4 °C and then with secondary anti-rabbit IgG conjugated with Alexa 594 (diluted 1:500 in PBS, Life Technologies) for 90 min at room temperature. Cells were mounted with Vectashield kit (Vector Laboratories), and the images were photographed using a Zeiss microscope (Zeiss, Immersol 518F, ZEN 2012, blue edition). Using ImageJ program (NIH Image, Bethesda, MD), the numbers of SMI312 positive neurons were counted.

Quantification of Neurite Outgrowth. To measure the neurite outgrowth of P19, primary hippocampal neurons, and primary cortical neurons, wide-field fluorescence images from four fields in each well of 384-well plate were acquired on the ArrayScan V^{TI} HCS reader (Thermo Fisher Scientific) using a 10× objective lens, and the images were analyzed with the Neuronal Profiling BioApplication software (Thermo Fisher Scientific).

For the measurement of retina neuronal cells, the number and axonal length of neurons in nine consecutive nonoverlapping microscopic fields with areas of 13.55 mm^2 (total area 40.65 mm^2) were counted. Both the total number of cells and the numbers of cells that contains axon length less than 50 μm, axon length of 50−100 μm, axon length of 100−200 μm, and axon length of longer than 200 μm were counted.

Optic Nerve Crush. Male SD rats (8 weeks of age, weighing 200−250 g) were purchased from Samtako Bio Korea, Inc. (Osan, GyeongGi-Do, Korea). Rats were housed in a temperature-controlled (22−24 °C) and humidity-controlled environment under a 12 h light/dark cycle (light on at 08:00 and off at 20:00). Rats were given ordinary laboratory food and water ad libitum. Rats were randomly divided into two groups: sham-operated normal control (n = 3) and compound **7p** after optic nerve crush (n = 4). The animals were anesthetized by intraperitoneal injection of 50 mg/kg tiletamine plus zolazepam (Zoletil; Virbac, Carros, France) and 15 mg/kg xylazine hydrochloride (Rompun; Bayer, Leuverkeusen, Germany). The pupils were dilated with 1% tropicamide eye drops. Dissection of the conjunctiva was made with forcep toward the back of the eye to expose the retrobulbar optic nerve. The optic nerve was crushed with sharp forceps for 15 s at 2 mm behind connected optic head. A sham-operated normal control group was injected with saline using 30G needle intravitreously once in 4 days. The crushed group was injected with compound **7p** (0.22 μg in 5 μL per eye) prepared in 100 mM potassium phosphate buffer with 0.01 N HCl once in 4 days for 3 weeks.

Preparation of Optic Nerve Sections and Immunohistochemistry. Anterior segments of the eyeballs with optic nerve and the vitreous humor were removed. The eyeballs with optic nerve were isolated and fixed by soaking in 4% paraformaldehyde for 2 h. The fixed retinas were soaked in 30% sucrose solution prepared in PBS, pH 7.4, at 4 °C overnight for cryoprotection and embedded in O.C.T. compound (Tissue-tek) before freezing at −80 °C. Leica cryostat was used to section the retina (12 μm). The sections were washed with PBS three times and were incubated with 1% BSA (MP, Cellect BSA) and 3% goat serum (Vector) in PBS (1% BSA) (blocking solution) for 1 h at room temperature to block nonspecific protein binding. Then the sections were incubated with primary anti-GAP-43 BRN3α (polyclonal, 1:200, Novus Biologicals) antibody for overnight at 4 °C and then with secondary anti-rabbit IgG-conjugated with Vector 488 (diluted 1:500 in PBS, Life technologies) for 90 min at room temperature. Sections were mounted with a Vecta shield kit (Vector

Laboratories, Inc. Burlingame, CA), and the images were photographed usinga Zeiss microscope (Zeiss, Immersol 518F, ZEN 2012, blue edition). Using ImageJ program (NIH Image, Bethesda, MD), the numbers of GAP-43 positive axons extending 0.5 and 1 mm from the end of the crush site were counted.

Quantification of Axon Growth. For analysis of axon length, the number of GAP-43 positive axon was counted in the 0.5, 1, and 1.5 mm from the end of the crush site in sections. The axons were measured by using formula at which the counts were used to calculate and group the average number of axons per millimeter of nerve width (100 μm box size). Then neuronal axon length was measured by formula as described.[23]

$$\Sigma\alpha_d = \pi r^2[\text{average axon (mm)}]/t$$

where $\Sigma\alpha_d$ is the total number of axon-extending distance, t is the thickness, and r is the radius of the nerve.

Statistics. Significant differences among groups were determined using a program, Graphpad prism (version 5, GraphPad Software, Inc., La Jolla, California). All values are reported as mean $\pm$ standard error of the mean. Statistical significance was set at $p < 0.05$.

General Methods. All substances were purchased from Sigma-Aldrich and used as received. Purchased anhydrous MeOH was used without further purification. Analytical thin-layer chromatography was conducted on E. Merck TLC plates (silica gel 60 F$_{254}$, aluminum back). Silica gel 60 (230−400 mesh) for column chromatography was purchased from E. Merck. Melting points were measured with a Kofler block or Büchi B-545 melting point apparatus. The ^{1}H and ^{13}C NMR spectroscopic data were recorded in CDCl$_3$, DMSO-d_6, and CD$_3$OD solutions at ambient temperature with Avance II 400 (Bruker Biospin, Germany, 400 MHz for ^{1}H NMR and 100 MHz for ^{13}C NMR) and Ascend III 700 (Bruker Biospin, 700 MHz for ^{1}H NMR and 175 MHz for ^{13}C NMR). Chemical shifts were recorded as δ values in parts per million (ppm) and were indirectly referenced to tetramethylsilane by the solvent signal. Coupling constants (J) are reported in Hertz. Infrared spectra were recorded on a Nicolet 6700 FTIR spectrophotometer. Low-resolution mass spectra were measured on a Micromass Quattro Micro API (Waters, USA), whereas high-resolution mass spectra were recorded on LTQ Orbitrap XL (Thermo Scientific, USA) spectrometer. Characterization data for known compounds were consistent with literature values.

Representative Compounds and Their Synthesis Procedures. All of the compounds were synthesized via route A (**7i−k**, **7l−p**, and **7r−g**), route B (**l**, **7c−f**, and **7t−x**), route C (**7q**, **12e**, **17**, and **18**) except commercially available compounds (**7b**, **7g**, and **7h**).

*2-(N-(2-Methoxyphenyl)-4-methylphenylsulfonamido)-N-(4-methoxypyridin-3-yl)acetamide (**7p**) via Route A.* To stirred compound **2a** (10.0 g, 81.2 mmol) and K$_2$CO$_3$ (16.8 g, 122 mmol) in DMF (150 mL) was added tosyl chloride (16.3 g, 85.3 mmol). After being stirred at rt for 10 min, the reaction solution was quenched with water and extracted with EtOAc. The combined organic phases were washed with water and brine and dried over concentrated Na$_2$SO$_4$. The resulting solid was tritured with hexane, providing 15.0 g (67%) of N-(2-methoxyphenyl)-4-methylbenzenesulfonamide (**3a**) as a white solid. To stirred compound **3a** (15.0 g, 54.1 mmol) and K$_2$CO$_3$ (18.6 g, 135 mmol) was added dropwise ethyl bromoacetate (5.98 mL, 85.3 mmol). After stirring at rt for 2 h, the reaction solution was quenched with water and extracted with EtOAc. The organic layer was washed with water and brine three times, dried over Na$_2$SO$_4$, filtered, and concentrated to give 19.0 g (96%) of ethyl 2-(N-(2-methoxyphenyl)-4-methylphenylsulfonamido)acetate (**4a**) as a white solid.

To a solution of compound **4a** (19.0 g, 52.3 mmol) was added 2.5 N NaOH (63 μL, 157 mmol) at rt. The reaction mixture was heated to reflux for 6 h. After cooled to rt, the mixture was concentrated and diluted with EtOAc and H$_2$O. The aqueous layer was adjusted to pH 2 with 1 N HCl (aqueous), then the product was extracted with EtOAc. The combined organic layers were dried over Na$_2$SO$_4$, concentrated. The resulting residue was recrystallized from EtOAc and hexane to obtain 15.0 g (86%) of 2-(N-(2-methoxyphenyl)-4-methylphenylsulfonamido)acetic acid (**5a**) as a white solid. To a mixture of compound **5a** (0.5 g, 1.49 mmol), compound **6p** (185 mg, 1.49

mmol), and HATU in DMF (20 mL) was added triethylamine (416 μL, 2.98 mmol) at 0 °C. The reaction solution was allowed to stir at rt for 2 h. The reaction was quenched with H_2O and diluted with EtOAc. The organic layer was washed with water and brine, dried over Na_2SO_4, and concentrated. The residue was purified by flash chromatography (EtOAc/hexane, 1:1, v/v) to give 250 mg (38%) of compound **7p** as a white solid. mp 153.0 °C; ^{1}H NMR (700 MHz, CDCl₃, δ) 9.45 (s, 1H), 9.32 (s, 1H), 8.36 (d, J = 6.3 Hz, 1H), 7.58 (d, J = 7.7 Hz, 2H), 7.35 (t, J = 7.0 Hz, 1H), 7.31−7.29 (m, 3H), 6.99− 6.95 (m, 2H), 6.86 (d, J = 8.4 Hz, 1H), 4.36 (s, 2H), 4.12 (s, 3H), 3.47 (s, 3H), 2.46 (s, 3H); ^{13}C NMR (175 MHz, CDCl₃, δ) 166.59, 155.45, 154.21, 146.37, 143.78, 141.43, 134.96, 131.46, 130.34, 129.10, 127.74, 126.89, 124.23, 120.75, 111.92, 105.55, 55.95, 55.02, 54.70, 21.61; LRMS (ESI) m/z: 442.1 [M + H]⁺; HRMS (ESI) m/z: Calcd for [M + H]⁺ $C_{22}H_{24}N_3O_5S$: 442.1431; found: 442.1435.

N-(2,5-Dimethoxyphenyl)-2-(4-fluoro-N-(2-methoxyphenyl)-phenylsulfonamido)acetamide (12a) via Route B. A mixture of compound **2a** (0.98 mL, 8.7 mmol), compound **8** (2.0 g, 8.7 mmol), and K_2CO_3 (1.8 g, 13.1 mmol) in DMF (17.4 mL) was heated at 80 °C for 2 h. The reaction was quenched with H_2O and the solution was diluted with EA and washed with H_2O and brine. The organic layer was dried over Na_2SO_4, filtered, and concentrated. The resulting residue was purified by flash chromatography (EtOAc/hexane, 1:2, v/v) to give compound **1a** as a brown solid. To a solution of compound **10a** (20 mg, 0.06 mmol) and compound **11a** (13 mg, 0.07 mmol) in DCM (0.3 mL) was added pyridine (25.0 μL, 0.32 mmol). After 3 h at rt, the reaction was quenched with H_2O, and then the solution was diluted with DCM. The organic layer was washed with Cu-SO₄(aqueous), H_2O, and brine, dried over Na_2SO_4, filtered, and concentrated. The residue was purified by flash chromatography (EtOAc/hexane, 1:4, v/v) to obtain 22 mg (78%) of compound **12a** as a yellow solid. mp 148.4 °C; ^{1}H NMR (400 MHz, DMSO-d_6, δ) 9.25 (s, 1H), 7.75−7.72 (m, 3H), 7.46−7.33 (m, 4H), 7.01−6.98 (m, 3H), 6.64 (dd, J = 8.8, 2.8 Hz, 1H), 4.42 (s, 2H), 3.84 (s, 3H), 3.68 (s, 3H), 3.41 (s, 3H); ^{13}C NMR (175 MHz, DMSO-d_6, δ) 167.01, 165.79, 164.36, 156.03, 153.52, 143.29, 135.89, 135.89, 132.56, 130.93, 128.15, 127.15, 120.91, 116.61, 112.97, 112.44, 108.55, 107.34, 56.95, 56.18, 55.86; LRMS (ESI) m/z: 475.1 [M + H]⁺; HRMS (ESI) m/z: Calcd for [M + H]⁺ $C_{23}H_{24}FN_2O_6S$: 475.1334; found: 475.1336.

4-Chloro-N-(2-((2,5-dimethoxyphenyl)amino)-2-oxoethyl)-N-(2-methoxyphenyl)benzamide (17) via Route C. To a mixture of compound **2a** (246 mg, 2.0 mmol) and K_2CO_3 (345 mg, 2.5 mmol) in DMF (10 mL) was added compound **13** (417 mg, 2.4 mmol) at rt. The solution was allowed to stir at rt for 2 h. The reaction was quenched with H_2O, and the solution was diluted with EA and washed with H_2O and brine. The organic layer was dried over Na_2SO_4, filtered and concentrated. The resulting residue was purified by flash chromatography (EtOAc/hexane, 1:2, v/v) to give 497 mg (95%) of intermediate **15** as a white solid. After LC/MS analysis of intermediate **15**, to a solution of compound **15** (26.1 mg, 0.1 mmol) and compound **8** (25.7 mg, 0.1 mmol) in DMF (5 mL) was added K_2CO_3 (20.7 mg, 0.15 mmol). The solution was heated to 80 °C for 2 h. The reaction was quenched with H_2O, and then the solution was diluted with DCM. The organic layer was washed with H_2O and brine, dried over Na_2SO_4, filtered, and concentrated. The residue was purified by flash chromatography (EtOAc/hexane, 1:4, v/v) to obtain 40 mg (83%) of compound **17** as a white solid. mp 161.8 °C; ^{1}H NMR (400 MHz, DMSO-d_6, δ) 9.38 (s, 1H), 7.81 (s, 1H), 7.33−7.21 (m, 6H), 7.02− 6.96 (m, 2H), 6.85 (t, J = 7.6 Hz, 1H), 6.64 (dd, J = 8.8, 2.8 Hz, 1H), 4.77−4.74 (m, 1H), 4.25−4.20 (m, 1H), 3.81 (s, 3H), 3.73 (s, 3H), 3.69 (s, 3H); ^{13}C NMR (175 MHz, CDCl₃, δ) 166.43, 155.50, 153.99, 142.77, 139.52, 137.16, 132.45, 130.70, 129.31, 128.88, 128.04, 126.62, 121.08, 111.98, 111.53, 109.04, 106.20, 56.85, 55.82, 54.93, 54.82; LRMS (ESI) m/z: 455.1 [M + H]⁺; HRMS (ESI) m/z: Calcd for [M + H]⁺ $C_{24}H_{24}ClN_2O_5$: 455.1368; found: 455.1369.

N-(2-Ethoxyphenyl)-2-(N-(2-methoxyphenyl)-4-methylphenyl-sulfonamido)acetamide (1). mp 178.3 °C; ^{1}H NMR (400 MHz, CDCl₃): δ 9.56 (s, 1H), 8.36 (d, J = 8.0 Hz, 1H), 7.57 (d, J = 8.0 Hz, 1H), 7.51 (d, J = 7.6 Hz, 2H), 7.34−7.27 (m, 3H), 7.09 (t, J = 6.4 Hz, 1H), 6.99−6.97 (m, 3H), 6.79 (d, J = 1.2 Hz, 1H), 4.35 (s, 2H), 4.26

(q, J = 8.8, 6.8 Hz, 2H), 3.36 (s, 3H), 2.45 (s, 3H), 1.69 (t, J = 7.2 Hz, 3H); ^{13}C NMR (100 MHz, DMSO-d_6, δ) 166.36, 155.54, 147.60, 143.62, 135.66, 132.08, 130.35, 129.36, 127.41, 126.96, 126.74, 124.15, 120.41, 120.32, 119.40, 112.56, 111.96, 64.22, 55.10, 54.12, 20.97, 14.63; LRMS (ESI) m/z: 455.2 [M + H]⁺; HRMS (ESI) m/z: Calcd for [M + H]⁺ $C_{24}H_{27}N_2O_5S$: 455.1635; found: 455.1635.

N-(3-Methoxyphenyl)-2-(N-(2-methoxyphenyl)-4-methylphenyl-sulfonamido)acetamide (7b). mp 206.7 °C; ^{1}H NMR (700 MHz, CD₃OD): δ 7.60 (d, J = 7.7 Hz, 2H), 7.39−7.35 (m, 3H), 7.31 (dd, J = 7.7, 1.4 Hz, 1H), 7.24−7.22 (m, 2H), 7.02 (t, J = 7.7 Hz, 2H), 6.97 (t, J = 7.7 Hz, 1H), 6.71 (dd, J = 8.4, 2.8 Hz, 1H), 4.38 (s, 2H), 3.80 (s, 3H), 3.60 (s, 3H), 2.46 (s, 3H); ^{13}C NMR (175 MHz, CD₃OD, δ) 167.71, 160.21, 156.30, 144.11, 138.80, 136.02, 131.63, 130.15, 129.23, 129.12, 127.60, 120.63, 112.08, 112.03, 109.81, 105.71, 54.73, 54.33, 54.13, 20.05; LRMS (ESI) m/z: 441.1 [M + H]⁺; HRMS (ESI) m/z: Calcd for [M + H]⁺ $C_{23}H_{25}N_2O_5S$: 441.1479; found: 441.1482.

2-(N-(2-Methoxyphenyl)-4-methylphenylsulfonamido)-N-phenyl-acetamide (7c). mp 167.9 °C; ^{1}H NMR (400 MHz, CDCl₃, δ) 9.35 (s, 1H), 7.61 (dd, J = 21.2, 8.4 Hz, 4H), 7.38−7.33 (m, 5H), 7.15 (t, J = 7.2 Hz, 1H), 7.02 (d, J = 8.4 Hz, 1H), 6.95−6.89 (m, 2H), 4.25 (s, 2H), 3.87 (s, 3H), 2.48 (s, 3H); ^{13}C NMR (100 MHz, DMSO-d_6, δ) 166.36, 155.74, 143.10, 138.54, 136.84, 132.93, 129.91, 129.22, 128.72, 127.17, 126.91, 123.36, 123.36, 120.18, 119.03, 112.24, 55.21, 52.84, 20.96; LRMS (ESI) m/z: 411.1 [M + H]⁺; HRMS (ESI) m/z: Calcd for [M + H]⁺ $C_{22}H_{23}N_2O_4S$: 411.1373; found: 411.1386.

N-(2-Ethylphenyl)-2-(N-(2-methoxyphenyl)-4-methylphenyl-sulfonamido)acetamide (7d). mp 152.2 °C; ^{1}H NMR (400 MHz, DMSO-d_6, δ) 9.27 (s, 1H), 7.57 (d, J = 8.0 Hz, 2H), 7.40 (d, J = 8.0 Hz, 2H), 7.35−7.28 (m, 3H), 7.22−7.13 (m, 3H), 7.01 (d, J = 8.0 Hz, 1H), 6.93 (t, J = 7.6 Hz, 1H), 4.38 (s, 2H), 3.32 (s, 3H), 2.50−2.44 (m, 2H), 2.41 (s, 3H), 1.03 (t, J = 7.6 Hz, 3H); ^{13}C NMR (100 MHz, CD₃OD, δ) 170.19, 157.62, 145.59, 139.98, 137.14, 135.61, 133.10, 131.66, 130.57, 130.02, 129.07, 128.89, 127.92, 127.43, 127.00, 121.99, 113.50, 55.97, 55.51, 25.30, 21.50, 15.00; LRMS (ESI) m/z: 439.2 [M + H]⁺; HRMS (ESI) m/z: Calcd for [M + H]⁺ $C_{24}H_{27}N_2O_4S$: 439.1686; found: 439.1695.

N-(2-Fluorophenyl)-2-(N-(2-methoxyphenyl)-4-methylphenyl-sulfonamido)acetamide (7e). mp 141.3 °C; ^{1}H NMR (400 MHz, DMSO-d_6, δ) 9.69 (s, 1H), 7.90−7.86 (m, 1H), 7.56 (d, J = 8.4 Hz, 2H), 7.40 (d, J = 8.0 Hz, 2H), 7.34−7.23 (m, 3H), 7.17−7.14 (m, 2H), 7.00 (d, J = 7.6 Hz, 1H), 6.95 (t, J = 7.6 Hz, 1H), 4.43 (s, 2H), 3.43 (s, 3H), 2.41 (s, 3H); ^{13}C NMR (175 MHz, CDCl₃, δ) 166.98, 156.42, 153.49, 144.17, 135.03, 130.48, 130.27, 129.46, 128.23, 126.05, 124.77, 124.44, 122.11, 121.22, 115.02, 114.91, 112.36, 55.57, 55.55, 21.54; LRMS (ESI) m/z: 429.1 [M + H]⁺; HRMS (ESI) m/z: Calcd for [M + H]⁺ $C_{22}H_{22}FN_2O_4S$: 429.1279; found: 429.1283.

N-(2-Bromophenyl)-2-(N-(2-methoxyphenyl)-4-methylphenyl-sulfonamido)acetamide (7f). mp 186.7 °C; ^{1}H NMR (400 MHz, DMSO-d_6, δ) 9.45 (s, 1H), 7.75 (d, J = 8.0 Hz, 1H), 7.68 (dd, J = 8.0, 1.2 Hz, 1H), 7.56 (d, J = 8.4 Hz, 2H), 7.40−7.31 (m, 5H), 7.49−7.10 (m, 1H), 7.01−6.93 (m, 2H), 4.40 (s, 2H), 3.43 (s, 3H), 2.41 (s, 3H); ^{13}C NMR (100 MHz, CD₃OD, δ) 166.85, 155.69, 143.41, 136.09, 135.54, 132.64, 132.40, 130.12, 129.32, 128.13, 127.38, 126.90, 126.67, 125.01, 120.31, 112.40, 55.20, 53.33, 20.98; LRMS (ESI) m/z: 489.0, 491.0 [M + H]⁺; HRMS (ESI) m/z: Calcd for [M + H]⁺ $C_{22}H_{22}BrN_2O_4S$: 489.0478; found: 489.0480.

Methyl 2-(2-(N-(2-Methoxyphenyl)-4-methylphenylsulfonamido)-acetamido)benzoate (7g). mp 156.7 °C, ^{1}H NMR (700 MHz, CDCl₃, δ) 11.88 (s, 1H), 8.73 (d, J = 8.3 Hz, 1H), 8.08 (dd, J = 8.0, 1.3 Hz, 1H), 7.92 (dd, J = 7.8, 1.5 Hz, 1H), 7.54 (m, 3H), 7.31 (td, J = 8.3, 1.5 Hz, 1H), 7.26 (d, J = 8.0 Hz, 2H), 7.13 (t, J = 7.3 Hz, 1H), 7.00 (t, J = 7.2 Hz, 1H), 6.75 (d, J = 8.0 Hz, 1H), 4.42 (s, 2H), 4.08 (s, 3H), 3.27 (s, 3H), 2.43 (s, 3H); ^{13}C NMR (175 MHz, CDCl₃, δ) 168.27, 168.06, 155.42, 143.44, 140.52, 136.05, 134.22, 133.54, 130.92, 130.11, 129.06, 128.01, 127.32, 122.94, 120.95, 120.70, 116.29, 111.47, 55.14, 54.63, 52.61, 21.48; LRMS (ESI) m/z: 469.1 [M + H]⁺; HRMS (ESI) m/z: Calcd for [M + H]⁺ $C_{24}H_{25}N_2O_6S$: 469.1428; found: 469.1437.

N-(2,4-Dimethoxyphenyl)-2-(N-(2-methoxyphenyl)-4-methyl-phenylsulfonamido)acetamide (7h). mp 163.3 °C; ^{1}H NMR

(CDCl$_3$, 400 MHz, δ) 9.19 (s, 1H), 8.15 (d, J = 8.8 Hz, 1H), 7.59 (d, J = 10.4 Hz, 2H), 7.38 (dd, J = 8.0, 1.2 Hz, 1H), 7.35−7.27 (m, 3H), 6.97 (t, J = 8.0 Hz, 1H), 6.83 (dd, J = 8.4, 1.2 Hz, 1H), 6.54 (d, J = 2.4 Hz, 1H), 6.48 (dd, J = 8.8, 2.8 Hz, 1H), 4.34 (s, 2H), 3.99 (s, 3H), 3.81 (s, 3H), 3.43 (s, 3H), 2.45 (s, 3H); ^{13}C NMR (100 MHz, CDCl$_3$, δ) 166.37, 156.77, 155.86, 150.06, 143.75, 135.66, 132.07, 130.36, 129.24, 128.01, 127.25, 121.07, 120.89, 120.82, 111.93, 103.81, 98.91, 56.05, 55.55, 54.96, 54.71, 21.55; LRMS (ESI) m/z: 471.2 [M + H]$^+$; HRMS (ESI) m/z: Calcd for [M + H]$^+$ C$_{24}$H$_{27}$N$_2$O$_6$S: 471.1585; found: 471.1590.

N-(2-Ethoxybenzyl)-2-(N-(2-methoxyphenyl)-4-methylphenylsulfonamido)acetamide (7i). mp 143.6 °C; ^{1}H NMR (400 MHz, DMSO-d_6, δ) 8.12 (t, J = 4.0 Hz, 1H), 7.54 (d, J = 8.4 Hz, 2H), 7.38−7.27 (m, 4H), 7.20 (t, J = 6.4 Hz, 1H), 6.98−6.88 (m, 4H), 6.82 (t, J = 7.2 Hz, 1H), 4.23−4.20 (m, 4H), 4.03−3.98 (m, 2H), 3.36 (s, 3H), 2.40 (s, 3H), 1.31 (t, J = 6.8 Hz, 3H); ^{13}C NMR (100 MHz, CDCl$_3$, δ) 168.07, 157.03, 156.29, 143.91, 135.29, 135.29, 130.44, 130.23, 130.14, 128.75, 128.23, 127.99, 125.94, 121.30, 120.96, 120.33, 112.10, 111.07, 63.58, 54.97, 54.69, 54.46, 39.32, 31.59, 21.56, 14.13; LRMS (ESI) m/z: 469.1 [M + H]$^+$; HRMS (ESI) m/z: Calcd for [M + H]$^+$ C$_{25}$H$_{29}$N$_2$O$_5$S: 469.1792; found: 469.1796.

N-(1H-Imidazol-2-yl)-2-(N-(2-methoxyphenyl)-4-methylphenylsulfonamido)acetamide (7j). mp 215.8 °C; ^{1}H NMR (400 MHz, DMSO-d_6, δ) 11.75 (br, 1H), 11.14 (br, 1H), 7.54 (d, J = 8.4 Hz, 2H), 7.39−7.30 (m, 4H), 6.99−6.91 (m, 2H), 6.72 (s, 2H), 4.40 (s, 2H), 3.43 (s, 3H), 2.41 (s, 3H); ^{13}C NMR (100 MHz, DMSO-d_6, δ) 155.71, 143.11, 136.82, 132.86, 129.93, 129.24, 127.13, 126.99, 120.09, 112.22, 55.21, 52.14, 20.96; LRMS (ESI) m/z: 401.1 [M + H]$^+$; HRMS (ESI) m/z: Calcd for [M + H]$^+$ C$_{19}$H$_{21}$N$_4$O$_4$S: 401.1278; found: 401.1292.

2-(N-(2-Methoxyphenyl)-4-methylphenylsulfonamido)-N-(thiazol-2-yl)acetamide (7k). mp 187.2 °C; ^{1}H NMR (400 MHz, DMSO-d_6, δ) 12.06 (s, 1H), 7.54 (d, J = 8.0 Hz, 2H), 7.47 (d, J = 7.6 Hz, 1H), 7.39 (d, J = 8.0 Hz, 3H), 7.32 (t, J = 8.8 Hz, 1H), 7.23 (d, J = 7.6 Hz, 1H), 6.99−6.93 (m, 2H), 4.49 (s, 2H), 3.40 (s, 3H), 2.41 (s, 3H); ^{13}C NMR (100 MHz, DMSO-d_6, δ) 166.95, 155.64, 143.20, 137.62, 136.63, 132.91, 129.99, 129.24, 127.13, 126.95, 120.19, 113.61, 112.22, 55.18, 52.14, 20.96; LRMS (ESI) m/z: 418.1 [M + H]$^+$; HRMS (ESI) m/z: Calcd for [M + H]$^+$ C$_{19}$H$_{20}$N$_3$O$_4$S$_2$: 418.0890; found: 418.0892.

2-(N-(2-Methoxyphenyl)-4-methylphenylsulfonamido)-N-(quinolin-3-yl)acetamide (7l). mp 177.0 °C; ^{1}H NMR (700 MHz, CDCl$_3$, δ) 10.35 (s, 1H), 9.05 (s, 1H), 8.64 (s, 1H), 7.95 (d, J = 8.4 Hz, 1H), 7.86 (d, J = 8.4 Hz, 1H), 7.70 (t, J = 7.7 Hz, 1H), 7.66 (d, J = 7.7 Hz, 2H), 7.54 (t, J = 7.0 Hz, 1H), 7.34 (t, J = 7.0 Hz, 1H), 7.32 (d, J = 7.7 Hz, 2H), 6.97−6.93 (m, 2H), 4.40 (s, 2H), 3.81 (s, 3H), 2.45 (s, 3H); ^{13}C NMR (175 MHz, CDCl$_3$, δ) 167.07, 156.34, 145.04, 144.32, 143.60, 134.34, 130.95, 130.51, 129.50, 129.03, 128.80, 128.38, 128.14, 127.93, 127.61, 127.05, 123.60, 121.63, 113.05, 56.49, 55.58, 21.68; LRMS (ESI) m/z: 462.1 [M + H]$^+$; HRMS (ESI) m/z: Calcd for [M + H]$^+$ C$_{25}$H$_{24}$N$_3$O$_4$S: 462.1482; found: 462.1491.

2-(N-(2-Methoxyphenyl)-4-methylphenylsulfonamido)-N-(quinolin-5-yl)acetamide (7m). mp 195.0 °C; ^{1}H NMR (700 MHz, CDCl$_3$, δ) 9.92 (s, 1H), 9.00 (s, 1H), 8.63 (d, J = 8.4 Hz, 1H), 8.11 (d, J = 8.4 Hz, 1H), 7.96 (d, J = 7.7 Hz, 1H), 7.66 (t, J = 8.4 Hz, 1H), 7.68 (d, J = 7.7 Hz, 2H), 7.60−7.58 (m, 1H), 7.41−7.37 (m, 3H), 7.00−6.98 (m, 3H), 4.35 (br, 2H), 3.64 (s, 3H), 2.50 (s, 3H); ^{13}C NMR (175 MHz, CDCl$_3$, δ) 167.27, 156.25, 150.28, 148.44, 144.27, 134.35, 132.03, 130.47, 130.10, 129.51, 129.41, 129.00, 128.48, 127.93, 127.18, 122.72, 121.38, 121.16, 121.04, 112.59, 55.88, 55.74, 21.68; LRMS (ESI) m/z: 462.1 [M + H]$^+$; HRMS (ESI) m/z: Calcd for [M + H]$^+$ C$_{25}$H$_{24}$N$_3$O$_4$S: 462.1482; found: 462.1493.

2-(N-(2-Methoxyphenyl)-4-methylphenylsulfonamido)-N-(quinolin-6-yl)acetamide (7n). mp 177.0 °C; ^{1}H NMR (700 MHz, CDCl$_3$, δ) 9.78 (s, 1H), 8.86 (s, 1H), 8.80 (s, 1H), 8.12 (d, J = 8.4 Hz, 1H), 7.85 (d, J = 8.4 Hz, 1H), 7.68 (t, J = 7.0 Hz, 1H), 7.66 (d, J = 8.4 Hz, 2H), 7.58 (t, J = 7.0 Hz, 1H), 7.39 (t, J = 7.0 Hz, 1H), 7.38 (d, J = 7.7 Hz, 2H), 7.07 (d, J = 8.4 Hz, 1H), 6.98 (t, J = 7.7 Hz, 1H), 6.91 (d, J = 7.7 Hz, 1H), 4.34 (br, 2H), 3.97 (s, 3H), 2.48 (s, 3H); ^{13}C NMR (175 MHz, CDCl$_3$, δ) 167.25, 156.35, 150.48, 148.94, 144.47, 134.35, 131.03, 130.47, 130.10, 129.51, 129.41, 129.00, 128.48, 127.93, 127.18, 122.72, 121.38, 121.16, 121.04, 112.59, 55.88, 55.74, 21.78; LRMS

(ESI) m/z: 462.1 [M + H]$^+$; HRMS (ESI) m/z: Calcd for [M + H]$^+$ C$_{25}$H$_{24}$N$_3$O$_4$S: 462.1482; found: 462.1495.

2-(N-(2-Methoxyphenyl)-4-methylphenylsulfonamido)-N-(3-methoxypyridin-2-yl)acetamide (7o). mp 123.0 °C; ^{1}H NMR (700 MHz, CDCl$_3$, δ) 9.70 (s, 1H), 8.12 (d, J = 4.2 Hz, 1H), 7.60 (d, J = 7.7 Hz, 2H), 7.33−7.24 (m, 5H), 7.09 (dd, J = 8.4, 4.9 Hz, 1H), 6.95 (t, J = 7.7 Hz, 1H), 6.84 (d, J = 8.4 Hz, 1H), 4.44 (s, 2H), 4.04 (s, 3H), 3.47 (s, 3H), 2.46 (s, 3H); ^{13}C NMR (175 MHz, CDCl$_3$, δ) 155.50, 143.62, 141.27, 139.30, 131.57, 130.19, 129.03, 127.74, 126.97, 120.66, 119.68, 117.31, 111.77, 55.95, 55.09, 54.95, 21.60; LRMS (ESI) m/z: 442.1 [M + H]$^+$; HRMS (ESI) m/z: Calcd for [M + H]$^+$ C$_{22}$H$_{24}$N$_3$O$_5$S: 442.1431; found: 442.1429.

2-(N-(2-Methoxyphenyl)-4-methylphenylsulfonamido)-N-(2-methoxypyridin-3-yl)acetamide (7q). mp 122.0 °C; ^{1}H NMR (700 MHz, CDCl$_3$, δ) 9.29 (s, 1H), 8.54 (dd, J = 7.8, 1.4 Hz, 1H), 7.90 (dd, J = 5.0, 1.5 Hz, 1H), 7.57 (d, J = 8.2 Hz, 2H), 7.38 (dd, J = 7.8, 1.3 Hz, 1H), 7.33 (t, J = 7.9 Hz, 1H), 7.28 (d, J = 7.9 Hz, 2H), 6.98 (t, J = 7.3 Hz, 1H), 6.89 (dd, J = 7.7, 5.0 Hz, 1H), 6.83 (d, J = 8.2 Hz, 1H), 4.35 (s, 2H), 4.15 (s, 3H), 3.46 (s, 3H), 2.44 (s, 3H); ^{13}C NMR (175 MHz, CDCl$_3$, δ) 167.54, 155.86, 153.53, 143.93, 140.65, 135.50, 131.86, 130.48, 129.28, 128.05, 127.30, 126.88, 122.37, 121.01, 117.12, 112.08, 55.06, 54.82, 53.93, 21.52; LRMS (ESI) m/z: 442.2 [M + H]$^+$; HRMS (ESI) m/z: Calcd for [M + H]$^+$ C$_{22}$H$_{25}$N$_3$O$_5$S: 442.1431; found: 442.1434.

N-(2-Ethoxypyridin-3-yl)-2-(N-(2-methoxyphenyl)-4-methylphenylsulfonamido)acetamide (7r). mp 133.0 °C; ^{1}H NMR (700 MHz, CDCl$_3$, δ) 9.37 (s, 1H), 8.57 (d, J = 7.7 Hz, 1H), 7.89 (d, J = 4.9 Hz, 1H), 7.57 (d, J = 7.7 Hz, 2H), 7.51 (d, J = 7.7 Hz, 1H), 7.34 (t, J = 7.7 Hz, 1H), 6.99 (t, J = 7.7 Hz, 1H), 6.89 (t, J = 7.7 Hz, 1H), 6.82 (d, J = 8.4 Hz, 1H), 4.59 (q, J = 7.0 Hz, 2H), 4.36 (s, 2H), 3.39 (s, 3H), 2.45 (s, 1H), 1.64 (t, J = 7.0 Hz, 3H); ^{13}C NMR (175 MHz, CDCl$_3$, δ) 166.233, 161.24, 147.66, 143.81, 143.72, 135.42, 135.20, 129.28, 128.16, 127.69, 127.26, 124.01, 120.81, 119.73, 111.37, 106.24, 64.73, 52.89, 21.56, 15.07; LRMS (ESI) m/z: 456.2 [M + H]$^+$; HRMS (ESI) m/z: Calcd for [M + H]$^+$ C$_{23}$H$_{26}$N$_3$O$_5$S: 456.1588; found: 456.1591.

N-(2-Isopropoxypyridin-3-yl)-2-(N-(2-methoxyphenyl)-4-methylphenylsulfonamido)acetamide (7s). mp 124.0 °C; ^{1}H NMR (700 MHz, CDCl$_3$, δ) 9.38 (s, 1H), 8.58 (d, J = 7.0 Hz, 1H), 7.89 (d, J = 9.1 Hz, 1H), 7.57−7.55 (m, 1H), 7.34 (t, J = 7.0 Hz, 1H), 7.29−7.28 (m, 2H), 6.99 (t, J = 7.7 Hz, 1H), 6.87 (dd, J = 7.7, 4.9 Hz, 1H), 6.80 (d, J = 8.4 Hz, 1H), 7.39 (t, J = 7.0 Hz, 1H), 7.38 (d, J = 7.7 Hz, 2H), 7.07 (d, J = 8.4 Hz, 1H), 6.98 (t, J = 7.7 Hz, 1H), 6.91 (d, J = 7.7 Hz, 1H), 4.34 (br, 2H), 3.97 (s, 3H), 2.48 (s, 3H); ^{13}C NMR (175 MHz, CDCl$_3$, δ) 166.97, 155.25, 152.16, 143.32, 140.30, 135.57, 132.03, 130.12, 129.11, 127.16, 126.48, 126.37, 121.90, 120.06, 116.44, 112.37, 68.61, 55.08, 53.92, 21.90, 21.00; LRMS (ESI) m/z: 470.2 [M + H]$^+$; HRMS (ESI) m/z: Calcd for [M + H]$^+$ C$_{24}$H$_{28}$N$_3$O$_5$S: 470.1744; found:470.1753.

N-(2-Ethoxyphenyl)-2-(N-(3-methoxyphenyl)-4-methylphenylsulfonamido)acetamide (7t). mp 175.7 °C; ^{1}H NMR (700 MHz, CD$_3$OD, δ) 8.17 (d, J = 8.4 Hz, 1H), 7.55 (d, J = 7.7 Hz, 2H), 7.40 (d, J = 7.7 Hz, 2H), 7.13−7.09 (m, 3H), 7.06 (d, J = 8.4 Hz, 1H), 6.92 (t, J = 7.0 Hz, 1H), 6.89 (d, J = 9.1 Hz, 2H), 4.38 (s, 2H), 4.24 (q, J = 7.0 Hz, 2H), 3.79 (s, 3H), 2.47 (s, 3H), 1.61 (t, J = 7.0 Hz, 3H); ^{13}C NMR (175 MHz, CD$_3$OD, δ) 166.84, 159.78, 148.14, 144.58, 134.25, 132.13, 129.45, 129.40, 127.74, 126.73, 124.44, 120.28, 119.47, 114.09, 111.33, 64.40, 55.41, 54.57, 20.10, 13.99; LRMS (ESI) m/z: 455.2 [M + H]$^+$; HRMS (ESI) m/z: Calcd for [M + H]$^+$ C$_{24}$H$_{28}$N$_3$O$_5$S: 455.1635; found: 455.1640.

N-(2-Ethoxyphenyl)-2-(4-methyl-N-phenylphenylsulfonamido)acetamide (7u). mp 159.4 °C; ^{1}H NMR (400 MHz, CDCl$_3$, δ) 9.31 (s, 1H), 8.33 (d, J = 7.6 Hz, 1H), 7.51 (d, J = 8.0 Hz, 2H), 7.36−7.29 (m, 5H), 7.20−7.18 (m, 2H), 7.06 (t, J = 9.2 Hz, 1H), 6.94 (t, J = 9.2 Hz, 2H), 4.34 (s, 2H), 4.24 (q, J = 8.8, 6.8 Hz, 2H), 2.47 (s, 3H), 1.68 (t, J = 7.2 Hz, 3H); ^{13}C NMR (100 MHz, DMSO-d_6, δ) 165.64, 147.68, 143.98, 139.49, 134.36, 129.75, 129.11, 128.00, 127.78, 127.49, 126.81, 124.30, 120.38, 119.70, 111.99, 64.12, 54.38, 21.01, 14.64; LRMS (ESI) m/z: 425.2 [M + H]$^+$; HRMS (ESI) m/z: Calcd for [M + H]$^+$ C$_{23}$H$_{25}$N$_2$O$_4$S: 425.1530; found: 425.1544.

N-(2-Ethoxyphenyl)-2-(*N*-(2-fluorophenyl)-4-methylphenyl-sulfonamido)acetamide (**7v**). mp 162.3 °C; ^{1}H NMR (CDCl$_3$, 400 MHz, δ) 9.40 (s, 1H), 8.36 (dd, *J* = 8.8, 2.0 Hz, 1H), 7.60 (d, *J* = 8.4 Hz, 2H), 7.40−7.31 (m, 4H), 7.16 (t, *J* = 8.4 Hz, 1H), 7.10−7.05 (m, 2H), 6.97−6.93 (m, 2H), 4.31 (s, 2H), 4.25 (q, *J* = 7.2 Hz, 2H), 2.47 (s, 3H), 1.66 (t, *J* = 7.2 Hz, 3H); ^{13}C NMR (175 MHz, CDCl$_3$, δ) 165.71, 157.91, 147.76, 144.59, 134.46, 131.85, 130.81, 129.78, 127.87, 127.29, 124.80, 124.16, 120.79, 119.48, 117.13, 116.93, 111.04, 64.58, 55.28, 21.65, 14.93; LRMS (ESI) *m/z*: 443.1 [M + H]$^+$; HRMS (ESI) *m/z*: Calcd for [M + H]$^+$ C$_{23}$H$_{24}$FN$_2$O$_4$S: 443.1436; found: 443.1444.

2-((*N*-(2-Chlorophenyl)-4-methylphenyl)sulfonamido)-*N*-(2-ethoxyphenyl)acetamide (**7w**). mp 163.8 °C; ^{1}H NMR (700 MHz, CDCl$_3$, δ) 9.36 (s, 1H), 8.33 (dd, *J* = 7.9, 1.3 Hz, 1H), 7.60 (d, *J* = 8.2 Hz, 2H), 7.44 (dd, *J* = 7.7, 1.7 Hz, 1H), 7.37 (dd, *J* = 7.8, 1.6 Hz, 1H), 7.34−7.17 (m, 4H), 7.05 (td, *J* = 7.9, 1.5 Hz, 1H), 6.98−6.86 (m, 2H), 4.58−4.25 (m, 2H), 4.20 (s, 2H), 2.44 (s, 3H), 1.62 (t, *J* = 7.0 Hz, 3H); ^{13}C NMR (175 MHz, CDCl$_3$, δ) 165.93, 147.77, 144.52, 136.62, 135.06, 133.85, 132.71, 131.01, 130.19, 129.77, 128.08, 127.71, 127.31, 124.15, 120.79, 119.67, 111.03, 64.54, 55.39, 21.65, 14.99; LRMS (ESI) *m/z*: 460.1 [M + H]$^+$; HRMS (ESI) *m/z*: Calcd for [M + H]$^+$ C$_{23}$H$_{24}$ClN$_2$O$_4$S: 459.1140; found: 459.1144.

N-(2-Ethoxyphenyl)-2-((4-methyl-*N*-(*o*-tolyl)phenyl)-sulfonamido)acetamide (**7x**). Sticky oil; ^{1}H NMR (700 MHz, CDCl$_3$, δ) 9.35 (s, 1H), 8.35 (dd, *J* = 8.0, 1.4 Hz, 1H), 7.56 (d, *J* = 8.2 Hz, 2H), 7.29 (d, *J* = 8.0 Hz, 2H), 7.21 (dd, *J* = 3.6, 2.2 Hz, 2H), 7.10−7.08 (m, 1H), 7.05 (td, *J* = 7.9, 1.6 Hz, 1H), 6.95−6.90 (m, 2H), 6.82 (d, *J* = 7.9 Hz, 1H), 4.19 (q, *J* = 7.0 Hz, 2H), 4.12 (q, *J* = 7.1 Hz, 2H), 2.44 (s, 3H), 2.30 (s, 3H), 1.60 (t, *J* = 7.0 Hz, 3H); ^{13}C NMR (175 MHz, CDCl$_3$, δ) 166.11, 147.64, 144.44, 139.16, 138.44, 134.29, 131.80, 129.72, 128.84, 128.78, 128.27, 127.36, 126.75, 124.06, 120.77, 119.50, 110.97, 64.49, 56.94, 21.62, 18.67, 14.90; LRMS (ESI) *m/z*: 440.1 [M + H]$^+$; HRMS (ESI) *m/z*: Calcd for [M + H]$^+$ C$_{24}$H$_{27}$N$_2$O$_4$S: 439.1686; found: 439.1682.

2-(4-Chloro-*N*-(2-methoxyphenyl)phenylsulfonamido)-*N*-(2,4-dimethoxyphenyl)acetamide (**12b**). mp 168.4 °C; ^{1}H NMR (700 MHz, CDCl$_3$, δ) 9.08 (s, 1H), 8.16 (d, *J* = 8.8 Hz, 1H), 7.61 (d, *J* = 8.6 Hz, 2H), 7.46 (d, *J* = 8.6 Hz, 2H), 7.44 (dd, *J* = 7.8, 1.4 Hz, 1H), 7.34 (t, *J* = 7.1 Hz, 1H), 6.99 (t, *J* = 7.6 Hz, 1H), 6.82 (d, *J* = 8.3 Hz, 1H), 6.54 (d, *J* = 2.5 Hz, 1H), 6.48 (dd, *J* = 8.8, 2.5 Hz, 1H), 4.36 (s, 2H), 3.98 (s, 3H), 3.81 (s, 3H), 3.43 (s, 3H); ^{13}C NMR (175 MHz, CDCl$_3$, δ) 165.97, 156.85, 155.57, 149.95, 139.49, 137.21, 132.33, 130.66, 129.32, 128.88, 126.72, 121.05, 120.96, 120.76, 112.00, 103.97, 98.92, 56.05, 55.55, 54.96, 54.69; LRMS (ESI) *m/z*: 491.1 [M + H]$^+$; HRMS (ESI) *m/z*: Calcd for [M + H]$^+$ C$_{23}$H$_{24}$ClN$_2$O$_6$S: 491.1038; found: 491.1047.

2-(4-Bromo-*N*-(2-methoxyphenyl)phenylsulfonamido)-*N*-(2,5-dimethoxyphenyl)acetamide (**12c**). mp 166.9 °C; ^{1}H NMR (700 MHz, CDCl$_3$, δ) 9.31 (s, 1H), 8.05 (d, *J* = 2.9 Hz, 1H), 7.62 (d, *J* = 8.4 Hz, 2H), 7.53 (d, *J* = 8.4 Hz, 2H), 7.47 (d, *J* = 7.6 Hz, 1H), 7.34 (t, *J* = 7.8 Hz, 1H), 6.99 (t, *J* = 7.6 Hz, 1H), 6.88 (t, *J* = 9.5 Hz, 1H), 6.80 (t, *J* = 9.7 Hz, 1H), 6.62 (dd, *J* = 8.9, 2.9 Hz, 1H), 4.36 (s, 2H), 3.98 (s, 3H), 3.78 (s, 3H), 3.42 (s, 3H); ^{13}C NMR (175 MHz, CDCl$_3$, δ) 166.40, 155.48, 153.98, 142.77, 137.67, 132.45, 131.88, 131.60, 131.52, 131.00, 130.71, 129.38, 129.11, 128.03, 128.00, 126.59, 121.08, 111.98, 111.52, 109.04, 106.20, 56.85, 55.82, 54.94, 54.82; LRMS (ESI) *m/z*: 535.1, 537.1 [M + H]$^+$; HRMS (ESI) *m/z*: Calcd for [M + H]$^+$ C$_{23}$H$_{24}$BrN$_2$O$_6$S: 535.0533; found: 535.0543.

N-(2,5-Dimethoxyphenyl)-2-(4-methoxy-*N*-(2-methoxyphenyl)-phenylsulfonamido)acetamide (**12d**). mp 176.5 °C; ^{1}H NMR (700 MHz, CDCl$_3$, δ) 9.44 (s, 1H), 8.05 (d, *J* = 2.9 Hz, 1H), 7.61 (d, *J* = 8.8 Hz, 2H), 7.42 (d, *J* = 7.8 Hz, 1H), 7.32 (t, *J* = 7.8 Hz, 1H), 6.97 (t, *J* = 7.6 Hz, 1H), 6.94 (d, *J* = 8.8 Hz, 2H), 6.87 (d, *J* = 8.9 Hz, 1H), 6.82 (d, *J* = 8.3 Hz, 1H), 6.61 (dd, *J* = 8.9, 3.0 Hz, 1H), 4.34 (s, 2H), 3.98 (s, 3H), 3.87 (s, 3H), 3.78 (s, 3H), 3.46 (s, 3H); ^{13}C NMR (175 MHz, CDCl$_3$, δ) 166.91, 163.25, 155.82, 153.97, 142.90, 132.20, 130.37, 130.33, 130.09, 128.20, 127.33, 120.91, 113.80, 111.96, 111.64, 108.99, 106.27, 56.91, 55.81, 55.65, 55.06, 54.87; LRMS (ESI) *m/z*: 487.2 [M + H]$^+$; HRMS (ESI) *m/z*: Calcd for [M + H]$^+$ C$_{24}$H$_{27}$N$_2$O$_7$S: 487.1534; found: 487.1536.

N-(2,5-Dimethoxyphenyl)-2-(*N*-(2-methoxyphenyl)-4-(methylthio)phenylsulfonamido)acetamide (**12e**). mp 188.5 °C; ^{1}H NMR (400 MHz, DMSO-*d$_6$*, δ) 9.26 (s, 1H), 7.76 (s, 1H), 7.56 (d, *J* = 8.0 Hz, 2H), 7.43 (d, *J* = 8.8 Hz, 2H), 7.37−7.33 (m, 2H), 7.01−6.98 (m, 3H), 6.64 (dd, *J* = 9.2, 3.2 Hz, 1H), 4.38 (s, 2H), 3.84 (s, 3H), 3.68 (s, 3H), 3.41 (s, 3H), 2.55 (s, 3H); ^{13}C NMR (175 MHz, CDCl$_3$, δ) 166.71, 155.73, 154.00, 146.12, 142.86, 134.40, 132.28, 130.46, 128.21, 127.10, 124.93, 120.97, 111.95, 111.63, 109.06, 106.22, 56.91, 55.82, 54.99, 54.88, 14.84, 14.08; LRMS (ESI) *m/z*: 503.1 [M + H]$^+$; HRMS (ESI) *m/z*: Calcd for [M + H]$^+$ C$_{24}$H$_{27}$N$_2$O$_6$S$_2$: 503.1305; found: 503.1310.

2-(*N*-(2-Methoxyphenyl)-4-(methylthio)phenylsulfonamido)-*N*-(4-methoxypyridin-3-yl)acetamide (**12f**). mp 166.0 °C; ^{1}H NMR (400 MHz, DMSO-*d$_6$*, δ) 9.37 (s, 1H), 8.92 (s, 1H), 8.25 (d, *J* = 5.2 Hz, 1H), 7.57 (d, *J* = 8.4 Hz, 2H), 7.43 (d, *J* = 8.4 Hz, 2H), 7.36 (t, *J* = 7.6 Hz, 2H), 7.14 (d, *J* = 5.6 Hz, 1H), 7.02−6.94 (m, 2H), 4.43 (s, 2H), 3.92 (s, 3H), 3.44 (s, 3H), 2.55 (s, 3H); ^{13}C NMR (100 MHz, DMSO-*d$_6$*, δ) 166.84, 155.67, 146.65, 145.30, 142.45, 134.87, 132.38, 130.11, 127.68, 126.92, 124.95, 123.85, 120.32, 120.32, 112.37, 106.92, 55.93, 55.23, 13.98; LRMS (ESI) *m/z*: 474.1 [M + H]$^+$; HRMS (ESI) *m/z*: Calcd for [M + H]$^+$ C$_{22}$H$_{24}$N$_3$O$_5$S$_2$: 474.1152; found: 474.1157.

2-(4-Bromo-*N*-(2-methoxyphenyl)phenylsulfonamido)-*N*-(4-me-thoxypyridin-3-yl)acetamide (**12g**). mp 123.0 °C; ^{1}H NMR (400 MHz, DMSO-*d$_6$*, δ) 9.37 (s, 1H), 8.89 (s, 1H), 8.24 (d, *J* = 5.6 Hz, 1H), 7.82 (d, *J* = 6.8 Hz, 2H), 7.60 (d, *J* = 6.4 Hz, 2H), 7.38−7.32 (m, 2H), 7.12 (d, *J* = 5.6 Hz, 1H), 7.01−6.94 (m, 2H), 4.46 (s, 2H), 3.90 (s, 3H), 2.69 (s, 3H); ^{13}C NMR (100 MHz, DMSO-*d$_6$*, δ) 166.73, 155.55, 155.40, 146.70, 142.64, 138.62, 132.61, 131.93, 130.27, 129.22, 126.83, 126.56, 123.82, 120.36, 112.35, 106.91, 55.90, 55.14, 53.08; LRMS (ESI) *m/z*: 506.0, 508.0 [M + H]$^+$; HRMS (ESI) *m/z*: Calcd for [M + H]$^+$ C$_{21}$H$_{21}$BrN$_3$O$_5$S: 506.0380; found: 506.0386.

N-(2,5-Dimethoxyphenyl)-2-((2-methoxyphenyl)(4-methylbenzyl)amino)acetamide (**18**). mp 142.0 °C; ^{1}H NMR (400 MHz, CDCl$_3$, δ) 10.02 (s, 1H), 8.06 (s, 1H), 7.27 (d, *J* = 8.0 Hz, 2H), 7.06 (d, *J* = 8.4 Hz, 4H), 6.93 (d, *J* = 7.2 Hz, 1H), 6.85−6.81 (m, 2H), 6.59 (dd, *J* = 8.8, 2.8 Hz, 1H), 4.34 (s, 2H), 3.92 (s, 3H), 3.89 (s, 3H), 3.78 (s, 3H), 2.28 (s, 3H); ^{13}C NMR (175 MHz, CD$_3$OD, δ) 170.71, 153.88, 153.75, 142.90, 138.96, 136.67, 134.61, 128.56, 128.44, 127.64, 124.41, 121.98, 120.22, 111.36, 110.88, 107.94, 105.99, 59.05, 57.53, 55.48, 54.68, 54.54, 19.66; LRMS (ESI) *m/z*: 429.1 [M + H]$^+$; HRMS (ESI) *m/z*: Calcd for [M + H]$^+$ C$_{25}$H$_{29}$N$_2$O$_4$: 429.2127; found: 429.2130.

■ ASSOCIATED CONTENT

Ⓢ Supporting Information

The Supporting Information is available free of charge on the ACS Publications website at DOI: 10.1021/acs.jmed-chem.6b00015.

> ^{1}H and ^{13}C NMR spectra of compounds **1**, **7b−x**, **12a−g**, **17**, and **18**. (PDF)
> Structure information for compounds **7b−x**, **12a−g**, **17**, and **18**. (CSV)

■ AUTHOR INFORMATION

Corresponding Authors

*E-mail: smahn@dankook.ac.kr. Phone: 82-41-550-1433. Fax: 82-41-559-7899
*E-mail: ychoi@gstep.re.kr. Phone: 82-31-888-6972. Fax: 82-31-888-6979

Notes

The authors declare no competing financial interest.

■ ACKNOWLEDGMENTS

◼ ABBREVIATIONS USED

CNS, central nervous system; RGC, retina ganglion cell; GAP43, growth-associated protein 43; SD, Sprague−Dawley; HBSS, Hank's buffered salt solution

◼ REFERENCES

(1) Kim, W. Y.; Snider, W. D. Neuroscience. Overcoming inhibitions. *Science* **2008**, *322*, 869−872.

(2) Harel, N. Y.; Strittmatter, S. M. Can regenerating axons recapitulate developmental guidance during recovery from spinal cord injury? *Nat. Rev. Neurosci.* **2006**, *7*, 603−616.

(3) Baptiste, D. C.; Tighe, A.; Fehlings, M. G. Spinal cord injury and neural repair: focus on neuroregenerative approaches for spinal cord injury. *Expert Opin. Invest. Drugs* **2009**, *18*, 663−673.

(4) Mar, F. M.; Bonni, A.; Sousa, M. M. Cell intrinsic control of axon regeneration. *EMBO Rep.* **2014**, *15*, 254−263.

(5) He, Z. Intrinsic control of axon regeneration. *J. Biomed. Res.* **2010**, *24*, 2−5.

(6) Park, K. K.; Liu, K.; Hu, Y.; Smith, P. D.; Wang, C.; Cai, B.; Xu, B.; Connolly, L.; Kramvis, I.; Sahin, M.; He, Z. Promoting axon regeneration in the adult CNS by modulation of the PTEN/mTOR pathway. *Science* **2008**, *322*, 963−966.

(7) Liu, K.; Tedeschi, A.; Park, K. K.; He, Z. Neuronal intrinsic mechanisms of axon regeneration. *Annu. Rev. Neurosci.* **2011**, *34*, 131−152.

(8) Moore, D. L.; Blackmore, M. G.; Hu, Y.; Kaestner, K. H.; Bixby, J. L.; Lemmon, V. P.; Goldberg, J. L. KLF family members regulate intrinsic axon regeneration ability. *Science* **2009**, *326*, 298−301.

(9) Ruschel, J.; Hellal, F.; Flynn, K. C.; Dupraz, S.; Elliott, D. A.; Tedeschi, A.; Bates, M.; Sliwinski, C.; Brook, G.; Dobrindt, K.; Peitz, M.; Brustle, O.; Norenberg, M. D.; Blesch, A.; Weidner, N.; Bunge, M. B.; Bixby, J. L.; Bradke, F. Axonal regeneration. Systemic administration of epothilone B promotes axon regeneration after spinal cord injury. *Science* **2015**, *348*, 347−352.

(10) Cho, Y.; Sloutsky, R.; Naegle, K. M.; Cavalli, V. Injury-induced HDAC5 nuclear export is essential for axon regeneration. *Cell* **2013**, *155*, 894−908.

(11) Wurdak, H.; Zhu, S.; Min, K. H.; Aimone, L.; Lairson, L. L.; Watson, J.; Chopiuk, G.; Demas, J.; Charette, B.; Halder, R.; Weerapana, E.; Cravatt, B. F.; Cline, H. T.; Peters, E. C.; Zhang, J.; Walker, J. R.; Wu, C.; Chang, J.; Tuntland, T.; Cho, C. Y.; Schultz, P. G. A small molecule accelerates neuronal differentiation in the adult rat. *Proc. Natl. Acad. Sci. U. S. A.* **2010**, *107*, 16542−16547.

(12) Koprivica, V.; Cho, K. S.; Park, J. B.; Yiu, G.; Atwal, J.; Gore, B.; Kim, J. A.; Lin, E.; Tessier-Lavigne, M.; Chen, D. F.; He, Z. EGFR activation mediates inhibition of axon regeneration by myelin and chondroitin sulfate proteoglycans. *Science* **2005**, *310*, 106−110.

(13) Gregori-Puigjane, E.; Setola, V.; Hert, J.; Crews, B. A.; Irwin, J. J.; Lounkine, E.; Marnett, L.; Roth, B. L.; Shoichet, B. K. Identifying mechanism-of-action targets for drugs and probes. *Proc. Natl. Acad. Sci. U. S. A.* **2012**, *109*, 11178−11183.

(14) Ding, S.; Wu, T. Y.; Brinker, A.; Peters, E. C.; Hur, W.; Gray, N. S.; Schultz, P. G. Synthetic small molecules that control stem cell fate. *Proc. Natl. Acad. Sci. U. S. A.* **2003**, *100*, 7632−7637.

(15) Dwyer, D. S.; Dickson, A. Neuroprotection and enhancement of neurite outgrowth with small molecular weight compounds from screens of chemical libraries. *Int. Rev. Neurobiol.* **2007**, *77*, 247−289.

(16) Jones-Villeneuve, E. M.; McBurney, M. W.; Rogers, K. A.; Kalnins, V. I. Retinoic acid induces embryonal carcinoma cells to differentiate into neurons and glial cells. *J. Cell Biol.* **1982**, *94*, 253−262.

(17) McCormick, M. B.; Tamimi, R. M.; Snider, L.; Asakura, A.; Bergstrom, D.; Tapscott, S. J. NeuroD2 and neuroD3: distinct expression patterns and transcriptional activation potentials within the neuroD gene family. *Mol. Cell. Biol.* **1996**, *16*, 5792−5800.

(18) Farah, M. H.; Olson, J. M.; Sucic, H. B.; Hume, R. I.; Tapscott, S. J.; Turner, D. L. Generation of neurons by transient expression of neural bHLH proteins in mammalian cells. *Development* **2000**, *127*, 693−702.

(19) Usher, L. C.; Johnstone, A.; Erturk, A.; Hu, Y.; Strikis, D.; Wanner, I. B.; Moorman, S.; Lee, J. W.; Min, J.; Ha, H. H.; Duan, Y.; Hoffman, S.; Goldberg, J. L.; Bradke, F.; Chang, Y. T.; Lemmon, V. P.; Bixby, J. L. A chemical screen identifies novel compounds that overcome glial-mediated inhibition of neuronal regeneration. *J. Neurosci.* **2010**, *30*, 4693−4706.

(20) Buchser, W. J.; Slepak, T. I.; Gutierrez-Arenas, O.; Bixby, J. L.; Lemmon, V. P. Kinase/phosphatase overexpression reveals pathways regulating hippocampal neuron morphology. *Mol. Syst. Biol.* **2010**, *6*, 391.

(21) Nassar, A. E.; Kamel, A. M.; Clarimont, C. Improving the decision-making process in the structural modification of drug candidates: enhancing metabolic stability. *Drug Discovery Today* **2004**, *9*, 1020−1028.

(22) Chojnacki, A.; Weiss, S. Production of neurons, astrocytes and oligodendrocytes from mammalian CNS stem cells. *Nat. Protoc.* **2008**, *3*, 935−940.

(23) Leon, S.; Yin, Y.; Nguyen, J.; Irwin, N.; Benowitz, L. I. Lens injury stimulates axon regeneration in the mature rat optic nerve. *J. Neurosci.* **2000**, *20*, 4615−4626.